REGULAR ARTICLE

blood advances

Antileukemic properties of the kinase inhibitor OTSSP167 in T-cell acute lymphoblastic leukemia

Cory Seth Bridges,[1] Taylor J. Chen,[1] Monica Puppi,[1] Karen R. Rabin,[2] and H. Daniel Lacorazza[1]

[1]Department of Pathology & Immunology, Baylor College of Medicine, Houston, TX; and [2]Department of Pediatrics, Baylor College of Medicine, Texas Children's Hospital, Houston, TX

Key Points

- OTSSP167 has antileukemic properties in T-ALL by inducing cell cycle arrest and apoptosis.
- OTSSP167 controls leukemia burden in xenografts from patients with T-ALL and exhibits a synergistic effect with standard drug therapy.

Novel drugs are needed to increase treatment response in children with high-risk T-cell acute lymphoblastic leukemia (T-ALL). Following up on our previous report on the activation of the MAP2K7-JNK pathway in pediatric T-ALL, here we demonstrate that OTSSP167, recently shown to inhibit MAP2K7, has antileukemic capacity in T-ALL. OTSSP167 exhibited dose-dependent cytotoxicity against a panel of T-ALL cell lines with IC_{50} in the nanomolar range (10-50 nM). OTSSP167 induces apoptosis and cell cycle arrest in T-ALL cell lines, associated at least partially with the inhibition of MAP2K7 kinase activity and lower activation of its downstream substrate, JNK. Other leukemic T-cell survival pathways, such as mTOR and NOTCH1 were also inhibited. Daily intraperitoneal administration of 10 mg/kg OTSSP167 was well tolerated, with mice showing no hematological toxicity, and effective at reducing the expansion of human T-ALL cells in a cell-based xenograft model. The same dosage of OTSSP167 efficiently controlled the leukemia burden in the blood, bone marrow, and spleen of 3 patient-derived xenografts, which resulted in prolonged survival. OTSSP167 exhibited synergistic interactions when combined with dexamethasone, L-asparaginase, vincristine, and etoposide. Our findings reveal novel antileukemic properties of OTSSP167 in T-ALL and support the use of OTSSP167 as an adjuvant drug to increase treatment response and reduce relapses in pediatric T-ALL.

Introduction

T-cell acute lymphoblastic leukemia (T-ALL) is an aggressive hematological malignancy, representing about 15% of pediatric leukemia cases.[1,2] Although the 5-year event-free survival of childhood ALL has improved to more than 85% in most centers,[3] the prognosis of patients with refractory or relapsed T-ALL is dismal. Because relapsed leukemia remains the leading cause of cancer-related mortality in children,[4-8] it is necessary to develop alternative drugs with antileukemic capacity and low toxicity for these patients who are at high-risk.

The development of alternative therapies requires the identification of novel actionable targets. Genomic analysis of 675 pediatric patients with cancer revealed that the MAPK pathway was one of the most affected and potentially druggable events.[9] Within MAPK signaling, MAP2Ks activate the effector kinases (extracellular signal-regulated kinase 1/2 [ERK1/2]), c-JUN NH2-terminal protein kinase (JNK), ERK5, and p38 at the end of the cascade and regulate cell proliferation, differentiation,

Submitted 11 July 2022; accepted 11 October 2022; prepublished online on *Blood Advances* First Edition 18 November 2022. https://doi.org/10.1182/bloodadvances.2022008548.

The full-text version of this article contains a data supplement.

and survival.[10] Our group described aberrant activation of the kinase MAP2K7, a component of a 3-tier signaling cascade associated with epigenetic silencing of the transcription factor KLF4, in pediatric patients with T-ALL.[11] Because JNK is the sole substrate of MAP2K7, we initially studied the antileukemic properties of JNK inhibition using the JNK-IN-8 compound and 2 adenosine triphosphate (ATP)–competitor JNK inhibitors tested in phase I/II clinical trials.[12,13] Although JNK inhibition could control leukemia burden in a mouse model of T-ALL, their low specificity and potency prevented significant improvements in survival by reaching sustained therapeutic concentrations with minimal toxicity.[11,14] We recently studied the compound 5Z-7-oxozeaenol in T-ALL because this chemical compound inhibited MAP2K7 through a covalent reaction with cysteine 218.[15] Although more potent than JNK inhibitors, 5Z-7-oxozeaenol toxicity limited the capacity of this compound to control leukemia efficiently in preclinical mouse models.[16]

Although OTSSP167 was described as an inhibitor of the maternal embryonic leucine zipper kinase (MELK),[17,18] the analysis of kinome studies deposited in the Library of Integrated Network-based Cellular Signatures (LINCS) shows a broad spectrum of kinase inhibition. OTSSP167 has been described as anticarcinogenic in solid tumors, such as adrenocortical carcinoma, breast cancer, glioma, cervical cancer, teratoid/rhabdoid tumors, adenocarcinoma, and lung squamous cell carcinoma.[19-23] OTSSP167 has also been studied in blood cancers, such as chronic myeloid leukemia, B cell lymphoma, and chronic lymphocytic leukemia.[18,24] OTSSP167 has been tested in clinical trials, including a phase 1 study of solid metastatic tumors, a safety study of breast cancer, and 2 open trials to evaluate the bioavailability of oral OTSSP167 and intravenous administration in leukemia (acute myeloid leukemia, ALL, advanced myelodysplastic syndrome, myeloproliferative neoplasm, and chronic myeloid leukemia). We decided to study OTSSP167 in T-ALL because it was identified as a potential MAP2K7 inhibitor in the LINCS program. And most importantly, a small screen using a thermal shift assay revealed OTSSP167 among 9 compounds with strong binding and inhibition of MAP2K7 and potency within a submicromolar range.[25]

Here, we describe the antileukemic properties of OTSSP167 in pediatric T-ALL using cell lines and patient samples. We show that OTSSP167 is cytotoxic in T-ALL cells via the induction of G2/M and G1/S cell cycle arrest and apoptosis associated with the inhibition of MAP2K7 kinase activity. In vivo studies establish high tolerance in mice and a significant capacity to control leukemia burden in cell-based and patient-derived xenograft studies. Drug combination studies revealed synergistic effects of OTSSP167 combined with drugs used in standard therapy. Our study warrants further testing of OTSSP167 as an adjuvant agent in combination with standard chemotherapy in frontline therapy or as a salvage agent in refractory and relapsed leukemia.

Methods

T-ALL cell lines

T-ALL cell lines (MOLT-3, JURKAT, KOPT-K1, P12-Ichikawa, DND41, RPMI-8402, ALL-SIL, CCRF-CEM, LCL) were cultured in RPMI-1640 medium supplemented with 10% fetal bovine serum. Cells were tested for mycoplasma and authenticated using short tandem repeat fingerprinting every 6 months.

Cytotoxicity assays

Cell lines were plated in triplicates at a cell density of 2×10^4 cells per well (96-well plate) and cultured for 48 hours in the presence of OTSSP167 (MedChemExpress) or vehicle control (dimethyl sulfoxide [DMSO]). Cell viability was measured using CellTiter-Glo Luminescent Cell Viability Assay. The half-maximal inhibitory concentration (IC_{50}) was calculated using nonlinear regression analysis via GraphPad software.

Apoptosis was measured using the FITC Annexin V apoptosis detection kit (Becton-Dickinson #559763). DNA content was determined by nuclei staining with propidium iodine. Flow cytometry analysis was conducted using FACS Canto (Becton-Dickinson Bioscience) and FlowJo software (TriStar).

For drug combination, cells were plated with OTSSP167 and drugs used in remission induction (vincristine [VCN], L-asparaginase [ASNase], and dexamethasone [Dex]). Cytotoxicity was measured as described above, and the data were analyzed using Combenefit [32].

In vitro kinase assay

Purified human MAP2K7 (Origene, 320 nM) was preincubated with a dead-JNK2 fragment (350 nM) in the presence of different concentrations of OTSSP167 or vehicle for 30 minutes. Afterward, ATP (100 μM final concentration) was added to initiate kinase activity for 30 minutes. Kinase activity was measured as the generation of adenosine diphosphate (ADP) using the ADP-GLO kit (Promega #V6930), and luminescence was determined using a 96-well plate Luminoskan ascent reader.

Immunoblot analysis

Cells were lysed with sodium dodecyl sulfate (SDS) lysis buffer containing 10 mM Tris, pH 7.4, 1% SDS, and 1 mM PMSF and supplemented with Halt Protease and Phosphatase Inhibitor Cocktail (Thermo Fisher Scientific). Protein lysates were electrophoresed using SDS-polyacrylamide gel electrophoresis and transferred to a polyvinylidene difluoride membrane using the iBLOT system. Antibodies corresponding to the following target proteins were used at a 1:1000 dilution: MELK (#2274), phospho-MAP2K7 (#4171), MAP2K7 (#4172), phospho–stress-activated protein kinase/JNK (SAPK/JNK, clone 81E11, #4668), SAPK/JNK (#9252), phospho–activating transcription factor 2 (phospho-ATF2, #15411), ATF2 (#9226), poly (ADP-ribose) polymerase (PARP, #9542, 1:10 000 dilution), cleaved caspase-3 (#9664), phospho-H2AX (#9719), phospho-Cdc2 (#9111), Cdc2 (#9112), Cyclin B1 (#4138), checkpoint kinase 1 (CHK1, #2306), polo-like kinase 1 (#4513), phospho-S6 (#2215), S6 (#2217), Notch1 (#3608), and HES1 (#11988). Secondary antibodies crosslinked with horseradish peroxidase (anti-rabbit immunoglobulin G #7074 and anti-mouse immunoglobulin G #7076) were used for the respective primary antibodies at concentrations of 1:20 000 to 1:50 000. Loading control β-actin (#643807) crosslinked with horseradish peroxidase (BioLegend) was used at a 1:500 000 dilution. Protein detection was performed using West Femto Maximum Sensitivity Substrate (Thermo Fisher Scientific) and Amersham Hyperfilm ECL (GE Healthcare).

Activation of MAP2K7 in T-ALL cell lines

KOPT-K1 cells were treated with 400 mM sorbitol for 1 hour, then OTSSP167 (30, 60, 90 nM) was added for 3 hours, followed by cell lysis for immunoblot analysis.

Cell-based and patient-derived xenograft

Bone marrow samples from patients with T-ALL were collected during diagnosis at the Texas Children's Cancer and Hematology Center. Samples were collected after written informed consent was obtained from all patients under a research protocol approved by the institutional review board. Leukemic blasts were transplanted into 10-week-old female NSG mice (0.5-1.0 × 10^6 cells per mouse). Peripheral blood sampled from the tail vein was routinely monitored for human $CD45^+$ cells via flow cytometry. Human leukemic cells were collected from the femur, tibia, and spleen, examined for human CD45 surface antigen expression, and viably frozen. Finally, NSG mice were injected with T-ALL PDX cells (0.5 × 10^6) and randomized into 2 groups (administration of vehicle or 10 mg/kg OTSSP167) when leukemic cells reached 1% to 5% in the blood. Mice were monitored at the end of each week for expansion of human $CD45^+$ cells in the peripheral blood via flow cytometry.

To evaluate drug toxicity, OTSSP167 (10 mg/kg) was prepared in 10% DMSO and 90% of a 20% solution of sulfobutylether-β-cyclodextrin (SBE-β-CD) and administered intraperitoneally every day from Monday to Friday for 2 weeks, and mice were monitored for body weight and complete blood counts. To study the efficacy of OTSSP167 in inhibiting leukemic growth, NSG mice were transplanted with KOPTK-1 cells labeled with firefly luciferase (2.5 × 10^5) and treated with vehicle (DMSO/SBE-β-CD) or OTSSP167 (10 mg/kg). Leukemia progression was evaluated by measuring the bioluminescence at the end of each week using the IVIS Imaging System (Xenogen). Images were acquired in anesthetized mice 10 minutes after intraperitoneal injection with 50 mg/kg D-luciferin.

Reverse phase protein array (RPPA)

Cell lysates, serial dilutions of standards, and positive and negative controls were arrayed on nitrocellulose-coated slides (Grace Bio-Labs) using the Quanteriz 2470 Arrayer. Each slide was probed with a validated primary antibody plus a biotin-conjugated secondary antibody. Signal detection was amplified using an Agilent GenPoint staining platform and visualized by DAP colorimetric reaction. The slides were scanned, analyzed, and quantified to generate spot intensity using customized software (Array-Pro Analyzer, Media Cybernetics). Each dilution curve was fitted with a logistic model (RPPA SPACE developed at MD Anderson). The protein concentrations were then normalized for protein loading. The corrections factor was calculated and normalized across sets via replicates-based normalization using an invariant set of control samples to adjust for batch differences between identical controls.[26]

Statistical analysis

All sample sizes (n values) indicated in each figure legend correspond to independent biological replicates. Unpaired two-tailed Student *t* test was used for statistical analysis. *P* values were determined using GraphPad software. Results with a *P* value $<.05$ were considered statistically significant.

Results

OTSSP167 inhibits cell viability in human T-ALL cells by inducing apoptosis and G2/M cell cycle arrest

We investigated the role of OTSSP167 in T-ALL based on our report that pediatric patients showed an aberrant activation of the MAP2K7-JNK pathway and the information that the MELK inhibitor OTSSP167 inhibits MAP2K7.[11,25] Firstly, immunoblot analysis showed that MELK is expressed in T-ALL cell lines, with elevated expression in KOPT-K1, MOLT-3, and RPMI-8402 (Figure 1A). MAP2K7 is expressed in all T-ALL cell lines, as previously described by our group (Figure 1A).[11] Cell viability assays showed dose-dependent cytotoxicity of OTSSP167 in a panel of T-ALL cell lines, with IC_{50}s ranging from 10 nM (KOPT-K1) to 57 nM (DND-41) (Figure 1B-C). The IC_{50}s for T-ALL cell lines are summarized in Figure 1C. The specificity of OTSSP167 to leukemic cells was evaluated by comparing cell viability in KOPT-K1 cells with a nonleukemic lymphoblastoid cell line (LCL) (Figure 1D). Comparative analysis of MAP2K7-JNK inhibitors against the KOPT-K1 cell line demonstrated that OTSSP167 (IC_{50} 12 nM) is more potent than 5Z-7-Oxozeaenol (IC_{50} 0.81 μM) and JNK-IN8 (IC_{50} 8.55 μM) (Figure 1E).[11,16] This difference in potency was also evident in other cell lines, such as ALL-SIL and RPMI-8402 (supplemental Figure 1). Collectively, the compound OTSSP167 emerges as a powerful antileukemic agent in T-ALL.

To further investigate the cause of OTSSP167-induced cytotoxicity, we evaluated the induction of apoptosis through flow cytometric detection of annexin V. Treatment of T-ALL cells with OTSSP167 (15 nM, 48 hours) induced significant apoptosis, particularly in KOPT-K1 and ALL-SIL cells (Figure 2A-B). Cell lines with an IC_{50} more than 50 nM (eg, JURKAT and DND-41) do not show a significant increase in apoptosis because the dose of OTSSP167 was lower than their IC_{50}; however, higher OTSSP167 concentrations (50 and 100 nM) induced apoptosis in these cell lines (supplemental Figure 2). Immunoblot analysis revealed that OTSSP167 induces the cleavage of both PARP and caspase 3, especially in the cell lines showing a significant induction of annexin V in response to OTSSP167 treatment (Figure 2C). Similarly, proteomic analysis by RPPA of KOPT-K1, MOLT-3, and P12-Ichikawa cell lines treated with vehicle or OTSSP167 (15 nM for 48 hours) revealed increased cleavage of caspases of the extrinsic pathway of apoptosis and annexin V in response to OTSSP167 treatment (Figure 2D). The RPPA also shows deregulation of other cellular pathways (supplemental Figure 3).

OTSSP167 has been described to alter cell cycle progression in bladder cancer cells through G1/S arrest via the p53 pathway.[27] We used propidium iodide nuclear staining to determine the effect of OTSSP167 on the cell cycle of T-ALL cells. Incubation of T-ALL cell lines with 15 nM OTSSP167 for 48 hours increased the percentage of cells in the G2/M phase of the cell cycle in the cell lines with lower IC_{50} (Figure 3A-B; supplemental Figure 4). The cell cycle arrest is more significant at 50 nM OTSSP167 in most cell lines (supplemental Figure 5). Some T-ALL cell lines also show a concomitant G1 arrest associated with an increase in G1 and a reduction in cyclin E (supplemental Figures 5 and 6). Although immunoblot analysis showed OTSSP167 increased the phosphorylation of Cdc2 and cyclin B1 (Figure 3C), higher OTSSP167

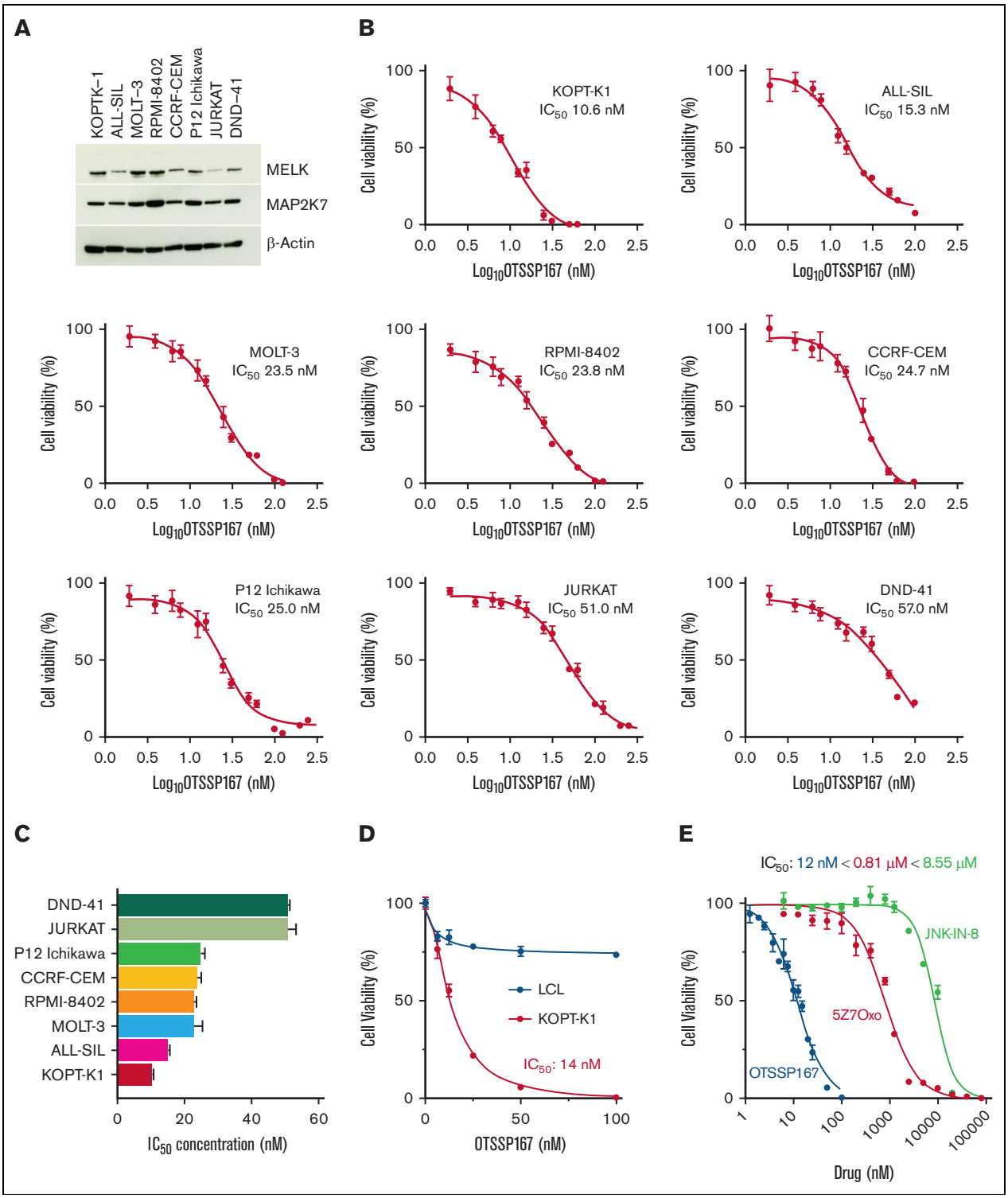

Figure 1. OTSSP167 inhibits cell viability in T-ALL cell lines. (A) Expression of MELK and MAP2K7 kinases in T-ALL cell lines. (B) Cell viability assays in T-ALL cell lines treated with OTSSP167 for 48 hours (n=3). IC_{50} is indicated for each cell line. Cell viability assays were averaged from 3 independent experiments performed in triplicates. (C) Potency of OTSSP167 in the panel of T-ALL cell lines. (D) Cytotoxicity in a leukemic cell line compared with an LCL (nonleukemic). (E) Comparative potency of JNK-IN-8, 5Z-7Oxozeaenol (5Z7O), and OTSSP167 in KOPT-K1 cells.

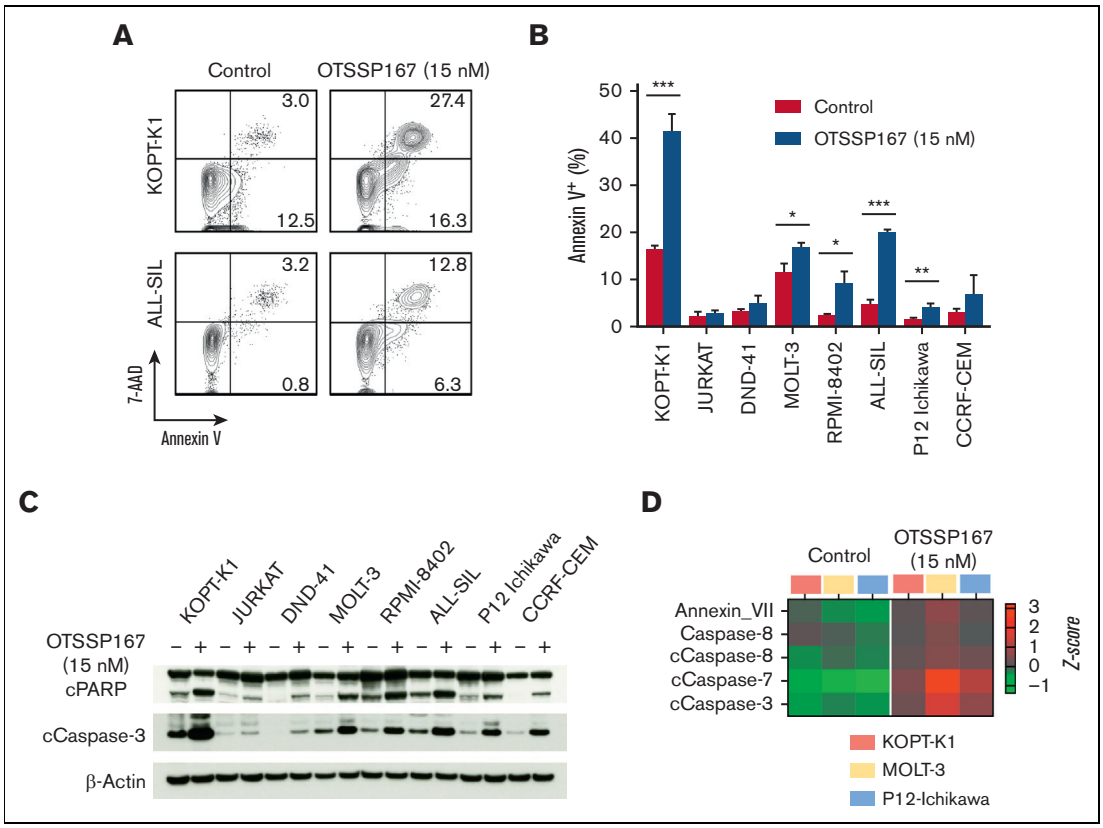

Figure 2. OTSSP167 induces cell death in T-ALL cell lines. (A) Representative flow cytometric analysis of annexin V staining for KOPT-K1 and ALL-SIL cell lines (15 nM OTSSP167, 48 hours). (B) Percentage of annexin V–positive cells upon OTSSP167 treatment (15 nM, 48 hours) is shown for all cell lines (n=3). The data represent 3 independent experiments and the mean and standard deviation. (C) Immunoblot analysis of cleaved PARP and caspase 3 in T-ALL cells treated with vehicle or 15 nM OTSSP167 for 48 hours. (D) Proteomic analysis by RPPA phase showing deregulation of proapoptotic proteins induced by treatment of KOPT-K1, MOLT-3, and P12-Ichikawa cell lines with OTSSP167 (15 nM, 48 hours). * $P < .05$, ** $P < .01$, *** $P < .001$ (two-tailed Student *t* test).

concentrations inhibited the phosphorylation of cyclin B1 (not shown). The RPPA analysis revealed an increase in H2AX with a reduction in several regulators of the G2/M checkpoint. A dose-dependent decrease of CHK1 and polo-like kinase 1 with an increase in phosphorylated H2AX was confirmed by immunoblots in the 3 cell lines (Figure 3E). Altogether, OTSSP167 induces DNA damage, cell cycle arrest, and apoptosis in T-ALL cell lines.

Inhibition of MAP2K7 by OTSSP167 in T-ALL

OTSSP167 is a MELK inhibitor that can also inhibit MAP2K7.[25] In addition to reducing MELK protein, OTSSP167 (50 nM) treatment substantially inhibited the phosphorylation of JNK and downstream ATF2 in all T-ALL cell lines (Figure 4A). Next, we investigated direct MAP2K7 inhibition in a biochemical assay using purified human MAP2K7 protein and dead-JNK2 as a substrate. The measurement of ADP production shows dose-dependent inhibition of MAP2K7 kinase activity with a 160 nM IC_{50}, within a low nanomolar range as previously reported (Figure 4B).[25] These data suggest that the observed cytotoxic effect may be mediated at least in part through MAP2K7 inhibition in T-ALL cells. To further support this model, we tested the capacity of OTSSP167 to inhibit MAP2K7 acutely activated by metabolic stress. Treatment of T-ALL cells with 400 mM sorbitol increases MAP2K7-mediated phosphorylation of JNK, which OTSSP167 inhibits in a dose-dependent manner (Figure 4C). Retroviral expression of the constitutively activated fusion protein MAP2K7-JNK2 in JURKAT and P12-Ichikawa cell lines (supplemental Figure 7) is inhibited by OTSSP167, further supporting that OTSSP167 can inhibit the MAP2K7 pathway in T-ALL cells (Figure 4D). The cytotoxicity of KOPT-K1 cells to OTSSP167 (IC50: 11 nM) and the MELK inhibitor MELK-8a (IC50: 10 μM), which has higher specificity to MELK than to OTSSP167,[28] suggests that low concentrations of OTSSP167 likely induce cell death in T-ALL cells independently of MELK inhibition (Figure 4E). Because OTSSP167 is a broad-spectrum kinase inhibitor, we performed an unbiased proteomic analysis of T-ALL cell lines treated with OTSSP167 to assess plasticity. RPPA analysis of T-ALL cells treated with 15 nM OTSSP167 revealed the inhibition of other cellular pathways with a critical role in T-ALL cells, such as mTOR and NOTCH1 (Figure 4F).[29-31] Immunoblot analysis of phosphorylated S6 and HES1 and downstream targets of mTOR and NOTCH1 confirmed that OTSSP167 inhibits phosphorylation of the ribosomal protein S6 and the levels of HES1 in T-ALL cells (Figure 4G). Interestingly, a low kinase specificity of OTSSP167 could have a therapeutic benefit in T-ALL by potentially targeting other pathways, in addition to MAP2K7-JNK, involved in the proliferation and survival of T-ALL cells.

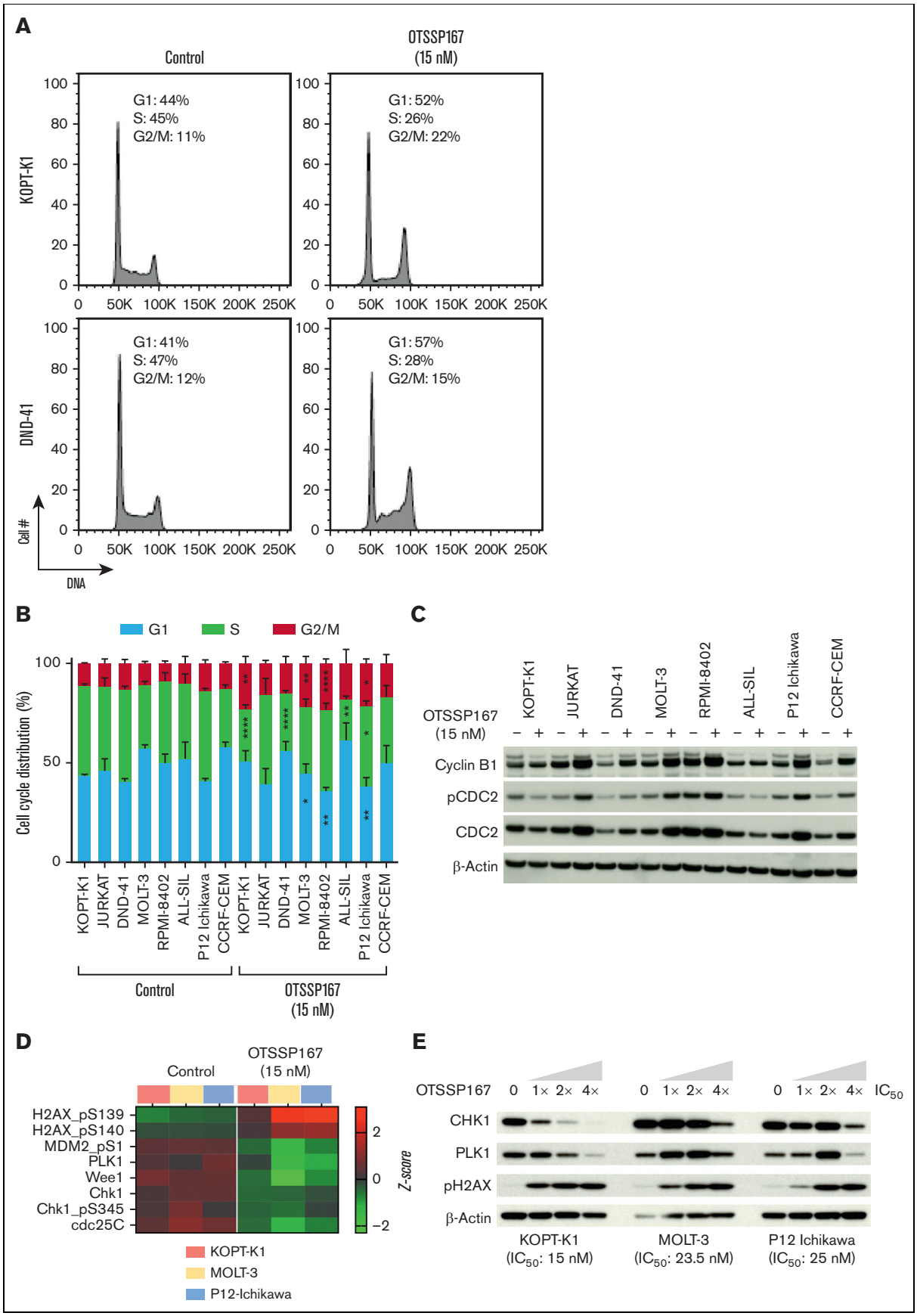
A
Control
OTSSP167 (15 nM)
KOPT-K1
DND-41
G1: 44%
S: 45%
G2/M: 11%
G1: 52%
S: 26%
G2/M: 22%
G1: 41%
S: 47%
G2/M: 12%
G1: 57%
S: 28%
G2/M: 15%
Cell #
DNA
B
G1
S
G2/M
Cell cycle distribution (%)
KOPT-K1
JURKAT
DND-41
MOLT-3
RPMI-8402
ALL-SIL
P12 Ichikawa
CCRF-CEM
Control
OTSSP167 (15 nM)
C
OTSSP167 (15 nM)
Cyclin B1
pCDC2
CDC2
β-Actin
D
Control
OTSSP167 (15 nM)
H2AX_pS139
H2AX_pS140
MDM2_pS1
PLK1
Wee1
Chk1
Chk1_pS345
cdc25C
Z-score
KOPT-K1
MOLT-3
P12-Ichikawa
E
OTSSP167
IC50
CHK1
PLK1
pH2AX
β-Actin
KOPT-K1 (IC50: 15 nM)
MOLT-3 (IC50: 23.5 nM)
P12 Ichikawa (IC50: 25 nM)

Figure 3.

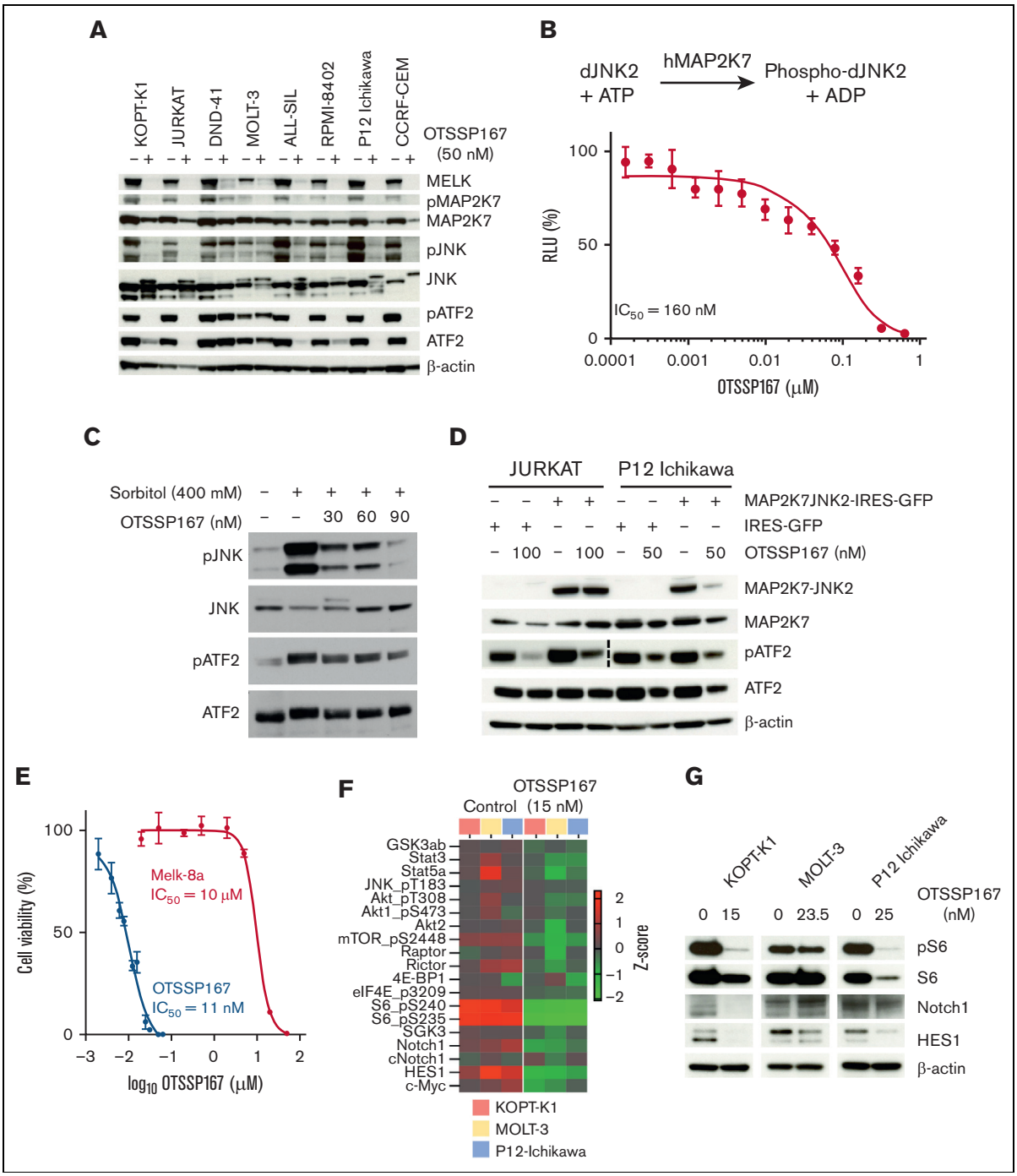

Figure 4. Inhibition of the MAP2K7-JNK pathway in T-ALL. (A) The inhibition of MELK and the MAP2K7-JNK pathway in T-ALL cell lines by OTSSP167 (50 nM, 48 hours) was analyzed by immunoblots. (B) Kinase activity was measured by incubating purified MAP2K7, dead-JNK2 (substrate), ATP (100 mM), and vehicle or OTSSP167 and measuring ADP consumption using ADP-Glo kit (n=3). (C) KOPT-K1 cells were treated with 400 mM sorbitol for 4 hours, and OTSSP167 was added for the last 3 hours. Inhibition of MAP2K7 was evaluated by detecting a reduction in phosphorylated JNK and ATF2 proteins. (D) OTSSP167 inhibited constitutive MAP2K7-JNK2 activation in JURKAT and P12-Ichikawa cells at 100 and 50 nM, respectively. (E) Cell viability of KOPT-K1 cells treated with OTSSP167 or MELK-8a. (F) Heatmap of the cell signaling pathways inhibited by OTSSP167 in T-ALL cell lines by RPPA. (G) Immunoblot analysis of inhibition of mTOR and NOTCH1 pathways by OTSSP167 in T-ALL cell lines.

Figure 3. OTSSP167 induces G2/M cell cycle arrest in T-ALL cell lines. (A) Representative flow cytometric analysis of DNA content (propidium iodide) of KOPT-K1 and DND-41 cell lines treated with vehicle or 15 nM OTSSP167 for 48 hours. (B) Effect of OTSSP167 treatment on the distribution in cell cycle phases in a panel of T-ALL cell lines (n=3). (C) Immunoblot analysis of regulators of the G2/M cell cycle checkpoint. (D) Heatmap showing alterations in the G2/M checkpoint by RPPA. (E) Immunoblot analysis of G2/M checkpoint regulators. * $P < .05$, ** $P < .01$, **** $P < .0001$ (two-tailed Student's *t* test).

In vivo antileukemic properties of OTSSP167 in human T-ALL

OTSSP167 is currently being tested in clinical trials for safety, bioavailability, and efficacy in solid tumors and hematological malignancies. Because of its broad inhibitory spectrum, we studied the toxicity of OTSSP167 before evaluating its effectiveness in T-ALL preclinical mouse models. C57BL/6 mice were administered Monday to Friday for 2 weeks and monitored for body weight to indicate general animal well-being and complete blood counts. Interestingly, OTSSP167 was well tolerated at a dose of 10 mg/kg without causing gross alterations in body weight (Figure 5A) or blood counts (Figure 5B). Next, we evaluated the efficacy of OTSSP167 in a cell-based xenograft model based on the injection of KOPT-K1 cells labeled with firefly luciferase into NSG mice that were randomized into 2 groups for treatment with vehicle (10% DMSO and 90% SBE-β-CD) and OTSSP167 (10 mg/Kg). Mice were monitored by whole-body bioluminescence imaging at the end of each week. The group treated with OTSSP167 showed a significant delay in the spread of leukemic cells (Figure 5C) and a considerable reduction of leukemia burden based on luminescence on days 14 and 21 of treatment (Figure 5D). Most importantly, mice treated with OTSSP167 showed a significantly prolonged survival (n=5, P=.0031) with a median survival of 36 days compared with 23 days in the control group (Figure 5E). Collectively, these data demonstrate the efficacy of OTSSP167 in controlling the expansion of leukemic cells in vivo with minimal toxicity.

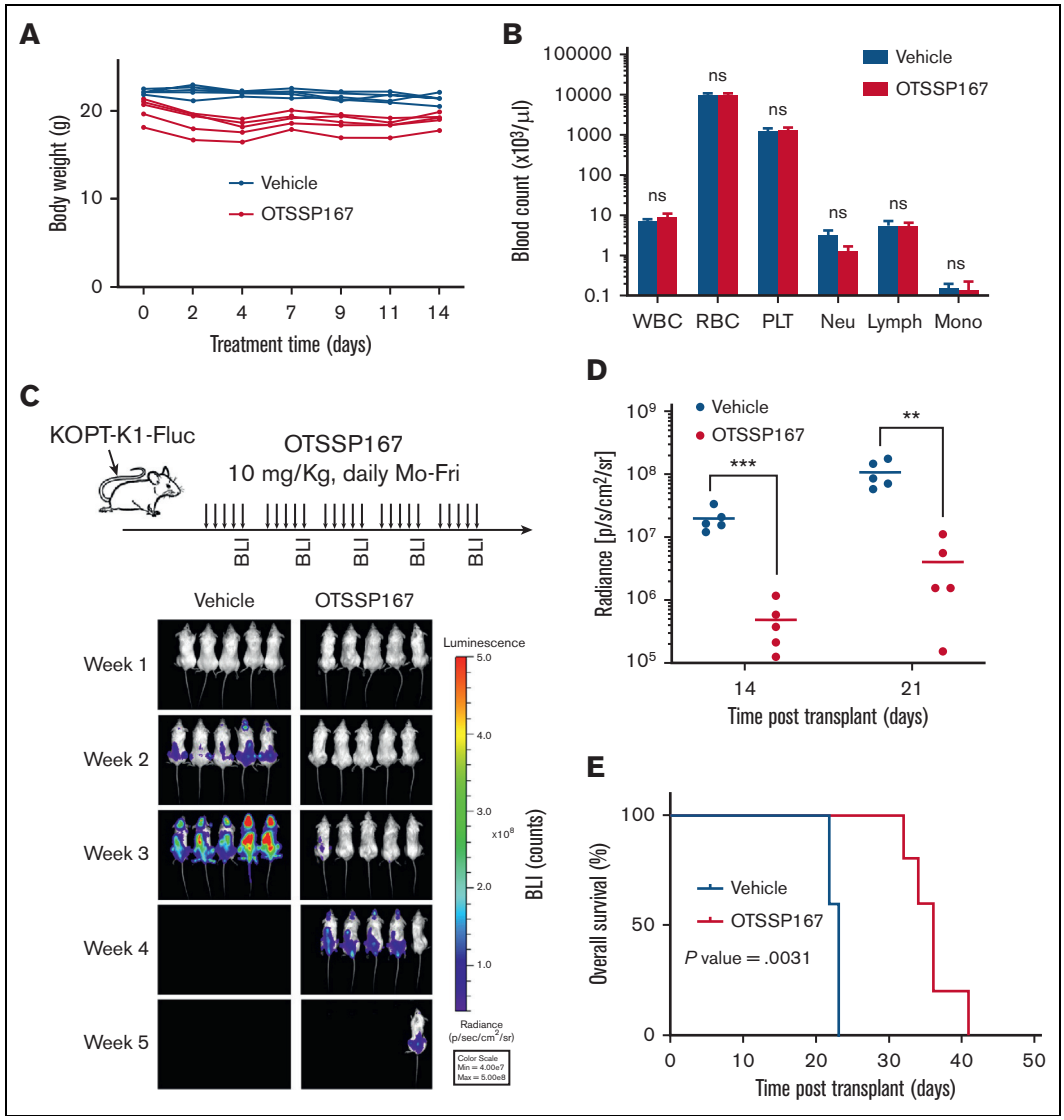

Figure 5. OTSSP167 inhibits the expansion of human T-ALL in a xenograft model. (A) Body weight monitoring of C57BL/6 mice treated Monday to Friday with vehicle or OTSSP167 (10 mg/kg) for 2 weeks. (B) Complete blood count at the end of the 2-week treatment. (C) KOPT-K1 cells labeled with firefly luciferase were injected into NSG mice and randomized into 2 groups for treatment with vehicle or OTSSP167 (10 mg/kg). At the end of each week, leukemia was monitored by BLI (n=5 per group). (D) Photon flux from BLI images at the end of weeks 2 and 3 of treatment. (E) Kaplan-Meier survival analysis. $^{**}P < .01$, $^{***}P < .001$ two-tailed Student t test was used in (D). Log-rank test was used in (E). BLI, bioluminescence imaging

The patient-derived xenograft (PDX) model is a preclinical model that closely correlates with clinical success. Hence, we tested OTSSP167 with a panel of T-ALL PDXs generated in our laboratory using lymphoblasts collected from children diagnosed with T-ALL leukemia at the Texas Children's Hospital and who entered remission or relapse (supplemental Figure 8). T-ALL PDX cells were injected into NSG mice and randomized into 2 groups when the human leukemic blasts were over 1% to 2% in peripheral blood. Treatment of PDX01 mice with OTSSP167 (10 mg/kg, Monday-Friday) for 3 weeks prevented the expansion of human leukemic blasts in blood compared with the vehicle control (Figure 6A-C). Despite treated mice showing a regrowth of T-ALL cells after discontinuing treatment, the overall survival improved significantly with a 3-week treatment regimen (Figure 6C-D). To evaluate the clearance of leukemic T cells in different tissues at the end of treatment, NSG mice carrying the PDX02 cells (relapsed T-ALL) were monitored during OTSSP167 treatment in blood and post mortem in the bone marrow and spleen. OTSSP167 controlled leukemia burden, and, in contrast to OTSSP167-treated mice, all mice administered with vehicle died during treatment, suggesting a similar survival as PDX01 (Figure 6E; supplemental Figure 9). At the end of drug administration, analysis of bone marrow showed an ~50% reduction of human $CD45^+$ cells in the bone marrow (Figure 6E) and a smaller spleen (supplemental Figure 9). Analysis of another PDX04 shows a similar control of leukemia burden during treatment with a significant reduction of human $CD45^+$ cells in the bone marrow (Figure 6F) and reduced splenomegaly (supplemental Figure 10). Figure 6G summarizes the leukemia burden at the end of treatment in the PDX model. Finally, the immunoblot analysis of phosphorylated JNK and HES1 in PDX01 and PDX04 cells treated in vitro with OTSSP167 shows inhibition of the MAP2K7 and NOTCH1 pathways (Figure 6H). Altogether, OTSSP167 can efficiently inhibit the expansion of patient T-ALL cells in vivo. Higher concentrations or longer treatments may be required to eliminate leukemic T cells in the bone marrow efficiently.

We evaluated the effect of combining OTSSP167 with drugs commonly used to treat pediatric T-ALL, such as VCN, ASNase, Dex, and etoposide.[5] This is critical because a new drug will be administered as an adjuvant rather than as a single agent. In P12-Ichikawa cells, we detected synergism between OTSSP167 and dexamethasone, analyzed using CompuSyn[32] and Combenefit visualization of drug interactions (supplemental Figure 11).[33] A synergistic effect of combining OTSSP167 with Dex, ASNase, or VCN was observed in KOPTK-1 cells (Figure 7A-C). Strikingly, a combination of OTSSP167 with a mixture of VCN, ASNase, and Dex displayed a strong synergism in KOPTK-1 cells, suggesting that OTSSP167 could be used in multidrug therapy (Figure 7D). The combination with etoposide was synergistic in MOLT-3 cell lines (Figure 7E). Finally, the specificity of OTSSP167 for leukemic cells was evaluated by comparing its cytotoxicity with that in normal bone marrow cells, which showed lower toxicity than normal blood cells (Figure 7F). Collectively, these data indicate that although the use of OTSSP167 is promising, further clinical studies are warranted.

Discussion

Identification of novel targets is necessary for developing targeted therapies for T-ALL. The prognosis has substantially improved for most patients with T-ALL through advances in risk assessment and intensified multidrug chemotherapy. However, the poor outcome of patients with refractory or relapsed disease supports the development of antileukemic drugs with high potency and low toxicity to withstand aggressive multidrug treatment regimens.

The genomic analysis of a large cohort of children with cancer identified MAPK signaling and cell cycle control as potentially druggable events.[9] Thus, the activation of kinase-driven signaling pathways in patients with leukemia warrants studies of pharmacological inhibition to control leukemia. For example, the tyrosine kinase inhibitor ponatinib has been investigated in relapsed/refractory Philadelphia chromosome–positive ALL.[34] PI3K/AKT is one of the most activated T-ALL pathways caused by PTEN mutations.[35] The finding that mutations in IL7R, JAK1, JAK3, or STAT5B activate the JAK-STAT pathway led to the clinical evaluation of the JAK inhibitor, ruxolitinib.[36,37] More recently, it was shown that the MAPK-ERK pathway is activated in IL7R-mediated steroid-resistant T-ALL, and therefore MEK inhibition with selumetinib enhances response to steroids.[38] Similarly, we described the activation of the kinase MAP2K7 via epigenetic silencing of KLF4 in pediatric T-ALL.[11] Thus, studies combining expression with genomic and epigenetic landscapes will reveal actionable pathways for therapeutic targeting not regulated through gene mutations.

MAP2K7 (also known as MKK7) is a dual-specificity mitogen-activated protein kinase that associates with its only downstream target, JNK.[10,39] An unidentified upstream MAP3K7 binds to MAP2K7-JNK, and this complex is held together by the scaffold JNK interacting protein. This pathway is activated by stress-associated signals, such as UV radiation, inflammation, metabolism, and the DNA damage response, which mediates the oncogenic stress stimuli to p53.[40] MAP2K7 is activated through phosphorylation of serine and threonine residues in the SKAKT motif in the kinase domain, whereas autoinhibition is controlled by the N-terminal regulatory helix.[41,42] The regulatory N-terminal domain of MAP2K7 contains 3 docking sites that recognize and bind JNK. Activated MAP2K7 phosphorylates the 3 isoforms, JNK1,JNK2 (both ubiquitous expressions), and JNK3 (expression limited to the brain, heart, and testis). JNK, in turn, activates cellular processes such as apoptosis and transcriptional regulation.[43,44] Early work shows JNK inhibition causes cell cycle arrest and apoptosis in JURKAT cells, and conversely, ectopic expression of fusion protein MAP2K7-JNK1 promotes cell cycle progression.[45] Our group later reported that genetic and epigenetic loss of the transcription factor KLF4 was associated with the aberrant activation of MAP2K7 in pediatric T-ALL and expansion of bulk leukemia and leukemia-initiating cells.[11] Consequently, pharmacological inhibition of the MAP2K7-JNK pathway would have antileukemic properties in T-ALL and potentially target leukemia-initiating cells.

This study evaluated the antileukemic properties of the MELK inhibitor OTSSP167 in T-ALL because of its capacity to inhibit MAP2K7.[25] Low nanomolar concentrations of OTSSP167 are cytotoxic in most T-ALL cell lines by deregulating the G2/M and G1/S checkpoints and inducing apoptosis. This alteration in the cell cycle is consistent with the arrest observed in *Map2k7*$^{-/-}$ mouse embryonic fibroblasts.[46] The inhibition of MAP2K7 kinase activity by OTSSP167, evaluated in a biochemical assay using full-length human MAP2K7 protein, shows an IC_{50} of 160 nM. This is consistent with a previous report showing OTSSP167 inhibits the

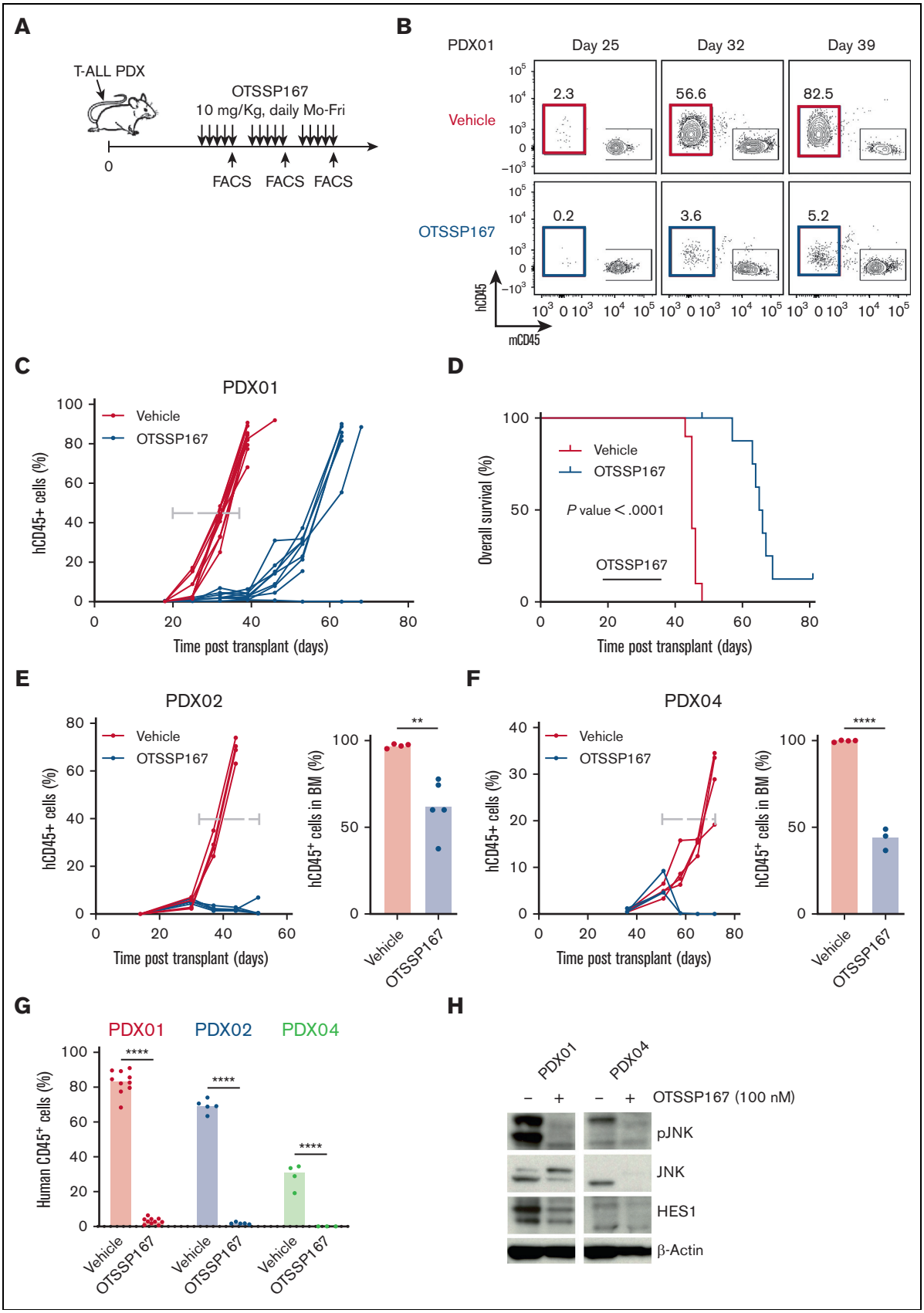

Figure 6. Efficacy to target in vivo patient-derived xenografts. (A) Diagram of treatment of T-ALL PDX mice with OTSSP167 (10 mg/kg) daily for 3 weeks. (B) Representative flow cytometric detection of human CD45 blasts at the end of each treatment week in T-ALL PDX01 (relapse) xenografts. (C) Monitoring human CD45 expansion in individual T-ALL PDX mice (PDX01) treated with vehicle or OTSSP167 (n= 10 per group). (D) Overall survival of mice from the experiment in

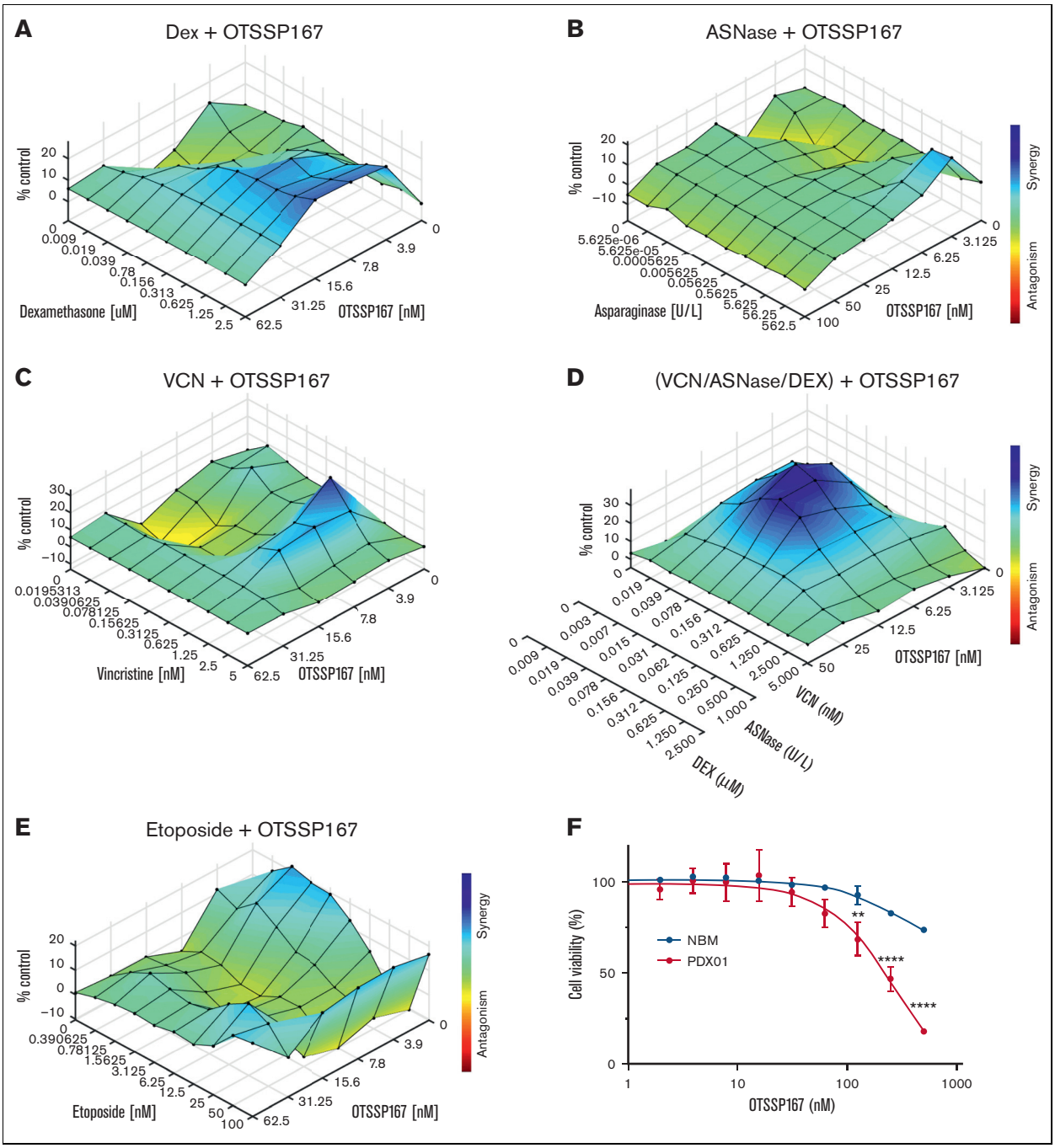

Figure 7. Combination of OTSSP167 with drugs used in remission induction. (A) Analysis of OTSSP167 combined with Dex in KOPTK-1 cells. (B) Analysis of OTSSP167 and ASNase combination in KOPTK-1 cells. The color bar representing the degree of synergism vs antagonism is the same as in (A). (C) Analysis of OTSSP167 combined with vincristine VCN in KOPTK-1 cells. (D) Analysis of OTSSP167 combined with a mixture of ASNase + DEX + VCN in KOPT-K1 cells. The color bar represents the degree of synergism vs antagonism as in (C). (E) Combination of OTSSP167 and etoposide in MOLT-3 cells. (F) Cytotoxicity of OTSSP167 to normal bone marrow cells compared with T-ALL PDX cells treated for 24 hours. $^{**}P < .01$, $^{****}P < .0001$ two-tailed Student *t* test was used in (F).

Figure 6 (continued) C (n= 10 per group, $P < .0001$). (E) Human CD45 expansion in individual T-ALL PDX mice (PDX02, relapse) treated with vehicle or OTSSP167 (n= 5 per group) during a 3-week treatment. Leukemia cells were analyzed in the bone marrow 2 days after the end of treatment. (F) Monitoring human CD45 expansion in individual T-ALL PDX mice (PDX04) treated with vehicle or OTSSP167 (n= 4 vehicle, n=3 OTSSP167) during a 3-week treatment. Leukemia cells were analyzed in the bone marrow 2 days after the end of treatment. (G) Percentage of human CD45 in blood at the end of a 3-week treatment for the 3 T-ALL PDXs. (H) Immunoblot analysis of inhibition of MAP2K7 and NOTCH1 pathways in T-ALL PDX01 and PDX04 treated with vehicle or 100 nM OTSSP167 for 17 hours. $^{**}P < .01$, $^{****}P < .0001$ two-tailed Student *t* test was used in (D). Log-rank test was used in (D).

phosphorylation mimetic mutant MAP2K7 S287D/T291D with an IC_{50} of 105 nM determined in an isothermal calorimetry and 60 nM in a kinase assay.[25] In this work, OTSSP167 was classified as a type-I inhibitor that binds to the highly flexible ATP-binding site.[25] The capacity to inhibit MAP2K7 was further supported by the inhibition of JNK phosphorylation in T-ALL treated with sorbitol to activate MAP2K7. In addition to MAP2K7 inhibition, OTSSP167 lowered the expression of MELK protein in the cell lines KOPT-K1, ALL-SIL, and RPMI-8402. This finding suggests a low specificity of OTSSP167 for MAP2K7. Analysis of KINOMEscan in the LINCS indicates a broad spectrum of kinase inhibition for a relatively high concentration of OTSSP167 (10 μM). These findings suggest that OTSSP167 is not a specific inhibitor but offers high potency and low toxicity, 2 highly desired features for clinical translation. Daily administration of OTSSP167 (10 mg/kg) showed good tolerability and efficient inhibition of leukemia expansion in cell-based and patient-derived xenograft models. In addition to T-ALL, identifying drugs that inhibit MAP2K7 will have broader applications because this pathway is activated in several solid tumors, such as breast, prostate, and glioma cancers.[47-50] Analysis of adult T-ALL gene expression shows higher MAP2K7 expression in patients with early immature leukemia.[51]

Our results demonstrate that kinase inhibition with OTSSP167 represents a potential therapeutic strategy for patients with T-ALL because of its high potency and low toxicity. Further studies are needed to evaluate OTSSP167 combined with current intensified chemotherapy in pediatric patients with T-ALL.

Acknowledgments

The authors thank Karen Prince for the preparation of figures and the design of the graphical abstract. This work was supported by the National Cancer Institute (RO1 CA207086-01A1) (H.D.L.), the ASH Bridge Award (H.D.L.), the National Institute of General Medical Sciences T32, National Institutes of Health (GM008231) (T.C.), the Cytometry and Cell Sorting Core at Baylor College of Medicine (P30 AI036211, P30 CA125123, and S10 RR024574), and the Flow Cytometry Core at Texas Children's Cancer and Hematology Center (S10 OD020066).

Authorship

Contribution: C.S.B. designed and performed experiments, interpreted the data, and contributed to manuscript preparation; T.C. contributed to MAP2K7 kinase assays and drug combination studies; M.P. generated animals for experiments; K.R.R. provided patient samples and revised the manuscript; and H.D.L. conceived, directed, and funded the project as the principal investigator.

Conflict-of-interest disclosure: The authors declare no competing financial interests.

ORCID profiles: C.S.B., 0000-0002-5200-2513; K.R.R., 0000-0002-4081-8195; H.D.L., 0000-0003-0660-617X.

Correspondence: H. Daniel Lacorazza, Texas Children's Hospital, 1102 Bates Ave, Feigin Tower, Suite 830, Houston, TX 77030; email: hdl@bcm.edu.

References

1. Pui CH, Robison LL, Look AT. Acute lymphoblastic leukaemia. *Lancet*. 2008;371(9617):1030-1043.
2. Siegel DA, Henley SJ, Li J, Pollack LA, Van Dyne EA, White A. Rates and trends of pediatric acute lymphoblastic leukemia - United States, 2001-2014. *MMWR Morb Mortal Wkly Rep*. 2017;66(36):950-954.
3. Teachey DT, Pui CH. Comparative features and outcomes between paediatric T-cell and B-cell acute lymphoblastic leukaemia. *Lancet Oncol*. 2019;20(3):e142-e154.
4. Pui CH, Carroll WL, Meshinchi S, Arceci RJ. Biology, risk stratification, and therapy of pediatric acute leukemias: an update. *J Clin Oncol*. 2011;29(5):551-565.
5. Pui CH, Evans WE. Treatment of acute lymphoblastic leukemia. *N Engl J Med*. 2006;354(2):166-178.
6. Iacobucci I, Mullighan CG. Genetic basis of acute lymphoblastic leukemia. *J Clin Oncol*. 2017;35(9):975-983.
7. Ko RH, Ji L, Barnette P, et al. Outcome of patients treated for relapsed or refractory acute lymphoblastic leukemia: a Therapeutic Advances in Childhood Leukemia Consortium study. *J Clin Oncol*. 2010;28(4):648-654.
8. Goldberg JM, Silverman LB, Levy DE, et al. Childhood T-cell acute lymphoblastic leukemia: the Dana-Farber Cancer Institute acute lymphoblastic leukemia consortium experience. *J Clin Oncol*. 2003;21(19):3616-3622.
9. Grobner SN, Worst BC, Weischenfeldt J, et al. The landscape of genomic alterations across childhood cancers. *Nature*. 2018;555(7696):321-327.
10. Pritchard AL, Hayward NK. Molecular pathways: mitogen-activated protein kinase pathway mutations and drug resistance. *Clin Cancer Res*. 2013;19(9):2301-2309.
11. Shen Y, Park CS, Suppipat K, et al. Inactivation of KLF4 promotes T-cell acute lymphoblastic leukemia and activates the MAP2K7 pathway. *Leukemia*. 2017;31(6):1314-1324.
12. Zhang T, Inesta-Vaquera F, Niepel M, et al. Discovery of potent and selective covalent inhibitors of JNK. *Chem Biol*. 2012;19(1):140-154.
13. Bennett BL, Sasaki DT, Murray BW, et al. SP600125, an anthrapyrazolone inhibitor of Jun N-terminal kinase. *Proc Natl Acad Sci U S A*. 2001;98(24):13681-13686.
14. Manning AM, Davis RJ. Targeting JNK for therapeutic benefit: from junk to gold? *Nat Rev Drug Discov*. 2003;2(7):554-565.
15. Sogabe Y, Matsumoto T, Hashimoto T, Kirii Y, Sawa M, Kinoshita T. 5Z-7-Oxozeaenol covalently binds to MAP2K7 at Cys218 in an unprecedented manner. *Bioorg Med Chem Lett*. 2015;25(3):593-596.

16. Chen TJ, Du W, Junco JJ, et al. Inhibition of the MAP2K7-JNK pathway with 5Z-7-oxozeaenol induces apoptosis in T-cell acute lymphoblastic leukemia. *Oncotarget*. 2021;12(18):1787-1801.
17. Chung S, Suzuki H, Miyamoto T, et al. Development of an orally-administrative MELK-targeting inhibitor that suppresses the growth of various types of human cancer. *Oncotarget*. 2012;3(12):1629-1640.
18. Zhang Y, Zhou X, Li Y, et al. Inhibition of maternal embryonic leucine zipper kinase with OTSSP167 displays potent anti-leukemic effects in chronic lymphocytic leukemia. *Oncogene*. 2018;37(41):5520-5533.
19. Kiseljak-Vassiliades K, Zhang Y, Kar A, et al. Elucidating the role of the maternal embryonic leucine zipper kinase in adrenocortical carcinoma. *Endocrinology*. 2018;159(7):2532-2544.
20. Meel MH, de Gooijer MC, Guillen Navarro M, et al. MELK inhibition in diffuse intrinsic pontine glioma. *Clin Cancer Res*. 2018;24(22):5645-5657.
21. Meel MH, Guillen Navarro M, de Gooijer MC, et al. MEK/MELK inhibition and blood-brain barrier deficiencies in atypical teratoid/rhabdoid tumors. *Neuro Oncol*. 2020;22(1):58-69.
22. Okur E, Yerlikaya A. A novel and effective inhibitor combination involving bortezomib and OTSSP167 for breast cancer cells in light of label-free proteomic analysis. *Cell Biol Toxicol*. 2019;35(1):33-47.
23. Ito M, Codony-Servat C, Codony-Servat J, et al. Targeting PKCiota-PAK1 signaling pathways in EGFR and KRAS mutant adenocarcinoma and lung squamous cell carcinoma. *Cell Commun Signal*. 2019;17(1):137-148.
24. Maes A, Maes K, Vlummens P, et al. Maternal embryonic leucine zipper kinase is a novel target for diffuse large B cell lymphoma and mantle cell lymphoma. *Blood Cancer J*. 2019;9(12):87.
25. Schroder M, Tan L, Wang J, et al. Catalytic domain plasticity of MKK7 reveals structural mechanisms of allosteric activation and diverse targeting opportunities. *Cell Chem Biol*. 2020;27(10):1285-1295.
26. Akbani R, Ng PK, Werner HM, et al. A pan-cancer proteomic perspective on The Cancer Genome Atlas. *Nat Commun*. 2014;5:3887.
27. Chen S, Zhou Q, Guo Z, et al. Inhibition of MELK produces potential anti-tumour effects in bladder cancer by inducing G1/S cell cycle arrest via the ATM/CHK2/p53 pathway. *J Cell Mol Med*. 2020;24(2):1804-1821.
28. McDonald IM, Grant GD, East MP, et al. Mass spectrometry-based selectivity profiling identifies a highly selective inhibitor of the kinase MELK that delays mitotic entry in cancer cells. *J Biol Chem*. 2020;295(8):2359-2374.
29. Weng AP, Ferrando AA, Lee W, et al. Activating mutations of NOTCH1 in human T cell acute lymphoblastic leukemia. *Science*. 2004;306(5694):269-271.
30. Sanchez-Martin M, Ferrando A. The NOTCH1-MYC highway toward T-cell acute lymphoblastic leukemia. *Blood*. 2017;129(9):1124-1133.
31. Khoshamooz H, Kaviani S, Atashi A, Mirpour Hassankiadeh SH. Combination effect of Notch1 and PI3K/AKT/mTOR signaling pathways inhibitors on T-ALL cell lines. *Int J Hematol Oncol Stem Cell Res*. 2020;14(2):99-109.
32. Chou TC, Talalay P. Quantitative analysis of dose-effect relationships: the combined effects of multiple drugs or enzyme inhibitors. *Adv Enzyme Regul*. 1984;22:27-55.
33. Di Veroli GY, Fornari C, Wang D, et al. Combenefit: an interactive platform for the analysis and visualization of drug combinations. *Bioinformatics*. 2016;32(18):2866-2868.
34. Yuda J, Yamauchi N, Kuzume A, Guo YM, Sato N, Minami Y. Molecular remission after combination therapy with blinatumomab and ponatinib with relapsed/refractory Philadelphia chromosome-positive acute lymphocytic leukemia: two case reports. *J Med Case Rep*. 2021;15(1):164.
35. Palomero T, Sulis ML, Cortina M, et al. Mutational loss of PTEN induces resistance to NOTCH1 inhibition in T-cell leukemia. *Nat Med*. 2007;13(10):1203-1210.
36. Kontro M, Kuusanmaki H, Eldfors S, et al. Novel activating STAT5B mutations as putative drivers of T-cell acute lymphoblastic leukemia. *Leukemia*. 2014;28(8):1738-1742.
37. Zenatti PP, Ribeiro D, Li W, et al. Oncogenic IL7R gain-of-function mutations in childhood T-cell acute lymphoblastic leukemia. *Nat Genet*. 2011;43(10):932-939.
38. van der Zwet JCG, Buijs-Gladdines J, Cordo V, et al. MAPK-ERK is a central pathway in T-cell acute lymphoblastic leukemia that drives steroid resistance. *Leukemia*. 2021;35(12):3394-3405.
39. Davis RJ. Signal transduction by the JNK group of MAP kinases. *Cell*. 2000;103(2):239-252.
40. Kotsinas A, Papanagnou P, Galanos P, et al. MKK7 and ARF: new players in the DNA damage response scenery. *Cell Cycle*. 2014;13(8):1227-1236.
41. Takekawa M, Tatebayashi K, Saito H. Conserved docking site is essential for activation of mammalian MAP kinase kinases by specific MAP kinase kinase kinases. *Mol Cell*. 2005;18(3):295-306.
42. Kinoshita T, Hashimoto T, Sogabe Y, Fukada H, Matsumoto T, Sawa M. High-resolution structure discloses the potential for allosteric regulation of mitogen-activated protein kinase kinase 7. *Biochem Biophys Res Commun*. 2017;493(1):313-317.
43. Dhanasekaran DN, Reddy EP. JNK signaling in apoptosis. *Oncogene*. 2008;27(48):6245-6251.
44. Kyriakis JM, Banerjee P, Nikolakaki E, et al. The stress-activated protein kinase subfamily of c-Jun kinases. *Nature*. 1994;369(6476):156-160.
45. Cui J, Wang Q, Wang J, et al. Basal c-Jun NH2-terminal protein kinase activity is essential for survival and proliferation of T-cell acute lymphoblastic leukemia cells. *Mol Cancer Ther*. 2009;8(12):3214-3222.

46. Wada T, Joza N, Cheng HY, et al. MKK7 couples stress signalling to G2/M cell-cycle progression and cellular senescence. *Nat Cell Biol*. 2004;6(3):215-226.

47. Wang Y, Xia Y, Hu K, et al. MKK7 transcription positively or negatively regulated by SP1 and KLF5 depends on HDAC4 activity in glioma. *Int J Cancer*. 2019;145(9):2496-2508.

48. Lotan TL, Lyon M, Huo D, et al. Up-regulation of MKK4, MKK6 and MKK7 during prostate cancer progression: an important role for SAPK signalling in prostatic neoplasia. *J Pathol*. 2007;212(4):386-394.

49. Hong L, Pan F, Jiang H, et al. miR-125b inhibited epithelial-mesenchymal transition of triple-negative breast cancer by targeting MAP2K7. *Onco Targets Ther*. 2016;9:2639-2648.

50. Zubor P, Hatok J, Moricova P, et al. Gene expression abnormalities in histologically normal breast epithelium from patients with luminal type of breast cancer. *Mol Biol Rep*. 2015;42(5):977-988.

51. Van Vlierberghe P, Ambesi-Impiombato A, De Keersmaecker K, et al. Prognostic relevance of integrated genetic profiling in adult T-cell acute lymphoblastic leukemia. *Blood*. 2013;122(1):74-82.